

**Technical Paper by S.K. Bhatia, J.L. Smith and
B.R. Christopher**

GEOTEXTILE CHARACTERIZATION AND PORE- SIZE DISTRIBUTION: PART III. COMPARISON OF METHODS AND APPLICATION TO DESIGN

ABSTRACT: Geotextiles are widely used in filtration applications. For continued growth in this area, it is critical that geotextiles be properly designed for these applications to prevent failures. The geotextile property that is most directly related to the design of a geotextile as a filter is the pore-size distribution of the geotextile. The main objective of this study was to compare the performance of the following six different test methods to evaluate the pore-size distribution of geotextiles: dry sieving, hydrodynamic sieving, wet sieving, bubble point method, mercury intrusion porosimetry, and image analysis. Twenty-eight geotextiles from five different manufacturers were evaluated. In this paper, the pore-size distribution results obtained from these methods are compared. The differences in pore opening results by different methods are illustrated using a design example.

KEYWORDS: Geotextile, Pore-Size distribution, Dry sieving, Hydrodynamic sieving, Wet sieving, Bubble point method, Mercury intrusion porosimetry, Image analysis, Geotextile filter.

AUTHORS: S.K. Bhatia, Associate Professor, Department of Civil and Environmental Engineering, Syracuse University, Syracuse, New York 13244, USA, Telephone: 1/315-443-3352, Telefax: 1/315-443-1243; J.L. Smith, Design Engineer, O'Brien & Gere Engineers, 5000 Brittonfield Parkway, Syracuse, New York 13221, USA, Telephone: 1/315-437-6100, Telefax: 1/315-463-7554; and B.R. Christopher, Consultant, 210 Boxelder Lane, Roswell, Georgia 30076, USA, Telephone: 1/770-641-8696, Telefax: 1/770-645-1383.

PUBLICATION: *Geosynthetics International* is published by the Industrial Fabrics Association International, 345 Cedar St., Suite 800, St. Paul, Minnesota 55101-1088, USA, Telephone: 1/612-222-2508, Telefax: 1/612-222-8215. *Geosynthetics International* is registered under ISSN 1072-6349.

DATES: Original manuscript received 14 September 1995, revised version received 3 April 1996 and accepted 6 April 1996. Discussion open until 1 March 1997.

REFERENCE: Bhatia, S.K., Smith, J.L. and Christopher, B.R., "Geotextile Characterization and Pore-Size Distribution: Part III. Comparison of Methods and Application to Design", *Geosynthetics International*, Vol. 3, No. 3, pp. 301-328.

1 INTRODUCTION

Geotextiles are widely used in filtration applications. For continued growth in this area, it is critical that geotextiles be properly designed for these applications to prevent failures. The geotextile property that is used in the design of a geotextile as a filter is its pore-size distribution; however, the design and selection of geotextile filters is not simple and designers are faced with many challenges. There are many similar geotextiles, however, they have completely different pore structures, as shown in Part I (Bhatia and Smith 1996a). There are also many different techniques for determining the pore-size distribution of geotextiles, and each technique may give different results for the same geotextile, as shown in Part II (Bhatia and Smith 1996b). Furthermore, there is a variety of filter criteria to select from, and different criteria can pass or fail a geotextile as a filter based on differences in the criteria and the use of pore openings measured using different techniques. A designer should select a filter criteria that takes into account the type of geotextile being used, that is based on a pore-size distribution method for which data is available, and that meets the anticipated application.

This paper is Part III of a three-paper series describing pore-size distribution characteristics of different types of geotextiles, methods for determining pore-size distribution, and the application of the pore-size distribution to the design of a geotextile as a filter. In this paper, the pore-size distribution results obtained by six different methods (dry sieving, hydrodynamic sieving, wet sieving, bubble point method, mercury intrusion porosimetry, and image analysis) are compared for a variety of geotextiles. The differences in pore opening results obtained by the six methods are discussed and illustrated with the help of a design example. For the design example, which only emphasizes pore-size characteristics of geotextiles in isolation, four different design criteria are used to further illustrate the differences between design criteria.

2 MATERIALS AND TEST METHODS

Twenty-eight geotextiles from five different manufacturers were selected for this study. Of the geotextiles selected, six are woven and twenty-two are nonwoven. The important physical properties of the geotextiles, such as, mass per unit area, thickness, apparent opening size (*AOS*), porosity, and fiber diameter are given in Table 1. The selected geotextiles are distinct in pore structure due to differences in manufacturing processes, as discussed in Part I (Bhatia and Smith 1996a).

The six test methods selected for this study are commonly used techniques for evaluating the pore-size distribution of geotextiles world-wide. These methods include dry sieving, hydrodynamic sieving, wet sieving, bubble point method, mercury intrusion porosimetry, and image analysis. A detailed discussion of these methods along with pore-size distribution results obtained by each method for the geotextiles selected are presented in Part II (Bhatia and Smith 1996b). As discussed in Part II, the six methods fall into four different categories and the results are not interchangeable (Bhatia et al. 1994; Fischer et al. 1996). A summary of differences between the six test methods is given in Table 2.

Table 1. The important physical properties of the geotextiles used in this study as determined by the authors (average values are given).

Geotextile	Mass/Area ⁽¹⁾ (g/m ²)	Thickness ⁽²⁾ (mm)	AOS (O_{95}) ⁽³⁾ (mm)	Porosity ⁽⁴⁾ (%)	Fiber diameter ⁽⁵⁾ (μ m)
Type A - Woven, slit-film, plain weave, PP					
A1	177	0.64	0.380	N/A	700-2500
A2	134	0.56	0.400	N/A	700-2500
A3	240	0.81	0.494	N/A	700-2500
A4	392	1.20	0.321	N/A	700-2500
Type A - Woven, multifilament, PET					
A5	360	0.73	0.346	N/A	20-29
A6	600	1.08	0.200	N/A	20-29
Type B - Nonwoven, needle-punched, staple fiber, PP					
B1	116	0.90	0.196	85.8	30-55
B2	159	1.06	0.142	83.4	30-55
B3	306	2.08	0.132	83.7	30-55
B4	377	3.13	0.139	86.6	30-55
B5	670	4.54	0.104	83.6	30-55
Type C - Nonwoven, needle-punched, continuous filament, PP					
C1	130	1.32	0.260	89.0	40-65
C2	220	2.04	0.162	88.0	40-65
C3	311	2.55	0.170	86.5	40-65
C4	444	3.50	0.150	85.9	40-65
C5	563	4.44	0.208	86.0	40-65
C6	431	3.46	0.217	86.2	40-65
Type D - Nonwoven, needle-punched, staple fiber, PET/PP					
D1	257	2.41	0.106	90.3	30
D2	322	2.72	0.102	89.2	30
D3	525	3.72	0.067	87.2	30
D4	185	1.57	0.143	89.3	30
D5	199	1.17	0.102	87.0	30
Type E - Nonwoven, heat-bonded, continuous filament, PP					
E1	58	0.34	0.571	81.2	30-70
E2	68	0.32	0.488	76.3	30-70
E3	106	0.39	0.193	69.9	30-70
E4	144	0.49	0.164	67.4	30-70
E5	215	0.61	0.097	60.8	30-70
E6	271	0.63	0.063	52.3	30-70

Notes: ⁽¹⁾ Average mass per unit area measured in accordance with ASTM D 3776. ⁽²⁾ Average thickness measured in accordance with ASTM D 1777. ⁽³⁾ Average AOS measured in accordance with ASTM D 4751. ⁽⁴⁾ Average porosity calculated based on specific gravity of PP = 0.9, PET = 1.3, and PET/PP = 1.1. ⁽⁵⁾ Average fiber diameter measured from photomicrographs of geotextiles taken with a scanning electron microscope. Unit conversions: 1 g/m² = 0.029 oz/yd²; 1 μ m = 0.001 mm; 1 mm = 39.37 mil = 0.039 inches. PP = polypropylene; PET = polyester.

Table 2. Comparison of pore-size distribution test methods.

Test method	Test mechanism	Test material	Data evaluation
Dry sieving	Sieving-dry	Glass bead fractions	Mass of glass beads passing
Hydrodynamic sieving	Alternating water flow	Glass bead mixtures/fractions	Wet sieve analysis
Wet sieving	Sieving-wet	Glass bead mixtures/fractions	Wet sieve analysis
Bubble point	Comparison of air flow dry versus saturated	Porewick	Calculated pore size versus filter flow
Mercury intrusion porosimetry	Intrusion of mercury into a pore	Mercury	Calculated pore size versus pore volume
Image analysis	Direct measurement of pores in a two dimensional plane	Not applicable	Projection into third dimension

3 COMPARISON OF RESULTS

In Part II (Bhatia and Smith 1996b), it was shown that pore-size distribution results for the selected geotextiles could be obtained by any of the six test methods included in this study. However, the results were not always a complete pore-size distribution, yet in most cases the O_{95} and O_{50} pore openings could be evaluated. The exceptions to this were the hydrodynamic and wet sieving tests using glass bead mixtures, which were only useful to evaluate O_{95} , and dry sieving results, which were only useful to the point where electrostatic effects were encountered.

In this paper, the pore-size distribution for the following four different types of geotextiles were obtained using each method and are compared:

- Slit-film, plain weave, woven geotextile A3.
- Staple fiber, needle-punched, nonwoven geotextile D1.
- Continuous filament, needle-punched, nonwoven geotextile C3.
- Continuous filament, heat-bonded, nonwoven geotextile E5.

3.1 Slit-Film, Plain Weave, Woven Geotextile A3

The slit-film, plain weave, woven geotextile, A3, showed a wide range in O_{95} , O_{50} , and O_{15} results, as shown in Figure 1 and Table 3. The hydrodynamic sieving and dry sieving methods gave the largest O_{95} pore openings, while the bubble point and mercury intrusion porosimetry methods gave the smallest.

The O_{50} and O_{15} pore openings of the woven geotextiles could not be measured using the dry or hydrodynamic sieving methods. It is believed that the dry sieving results beyond the range of O_{95} were inaccurate due to electrostatic effects and possible filament rotation and/or displacement of the woven geotextile during testing. In addition, the hydrodynamic sieving and wet sieving tests were developed primarily to provide information on the largest pore openings passing through the entire thickness of the geotextile.

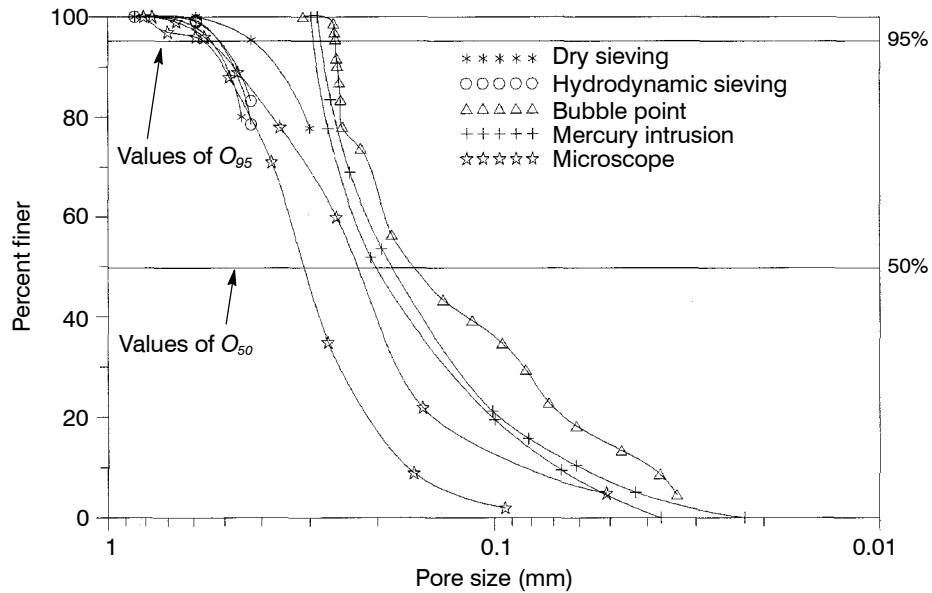


Figure 1. The complete pore-size distribution curves evaluated using each test method for slit-film, plain weave, woven geotextile A3.

Table 3. Average pore opening results using different test methods for the slit-film, plain weave, woven geotextile A3.

Pore opening	Dry sieving (mm)	Hydrodynamic sieving (mm)	Bubble point method (mm)	Mercury intrusion porosimetry (mm)	Microscope (mm)
O_{95}	0.494	0.511	0.263	0.285	0.560
O_{50}	N/A	N/A	0.170	0.194	0.270
O_{15}	N/A	N/A	0.0510	0.0810	0.150

Note: N/A = not applicable.

Therefore, glass bead mixtures were specified to better simulate soil particle interaction in the field and to also reduce the duration of the test. The results obtained by these methods, when glass bead mixtures are used, provide useful information on the larger pore openings of a geotextile, such as the O_{95} . However, since the remaining portion of the curve (O_{50} , O_{15}) is only a reflection of the gradation of the original glass bead mixture, the results beyond O_{95} are meaningless.

Since it was possible to directly measure the pore openings of geotextile A3, the pores were directly measured with a light microscope. The length and width of fifty pores in two different specimens were measured with a light microscope at $\times 20$ magnification. An effective circular diameter was calculated for each opening based on the smallest of the two measurements taken. The frequency of occurrence was used to evaluate the pore-size distribution of the geotextile. Microscope results for geotextile A3 are also

shown in Figure 1. The O_{95} values for the two specimens were in agreement; however, the O_{50} and O_{15} values were different. It is believed that the differences in O_{50} and O_{15} pore openings between the specimens are due to the variability in fine pore openings, and judgement and accuracy when measuring fine pores. Average O_{95} microscope measurements for this geotextile were approximately 0.56 mm.

Based on the ability to directly measure the pore openings of the geotextiles using a microscope, results obtained using the other methods are compared to the microscope results. The hydrodynamic sieving and dry sieving O_{95} values were approximately 10% lower than the microscope O_{95} results, and the bubble point and mercury intrusion O_{95} values were approximately 50% lower. The O_{50} mercury intrusion and bubble point values were approximately 30% lower than microscope results. In the range of O_{15} values, the mercury and bubble point results were approximately 55% lower than the microscope results. For the bubble point method, it is believed that these discrepancies were due to the low pressure required for fluid penetration. Improvement in the bubble point results may be realized by using a more viscous fluid other than porewick. Also, the direct measurement results may not be accurate in the smaller size range due to errors in judgement.

In the range of O_{95} values, the dry sieving and hydrodynamic sieving methods are believed to be more accurate for slit-film, plain weave, woven geotextiles than the other methods based on the closeness in O_{95} results to the microscope values. The wet sieving method was not performed with this geotextile; however, it is believed that it would provide similar results to hydrodynamic sieving. The overall shapes of the pore-size distribution curves given by the microscope were, however, more similar to those given by the bubble point and mercury intrusion methods. These trends were also exhibited for two other slit-film, plain weave geotextiles.

Both the mercury intrusion and bubble point methods were designed for fine pore size materials, yet, woven geotextiles have very large pore openings. In the mercury intrusion method, very little pressure is required to intrude the pores of a woven geotextile, and thus, at these low pressures, measurements may be inaccurate. In the bubble point method, very high flow rates are required for woven geotextiles. Measurements are not as accurate at high flow rates as compared to low flow rates; therefore, mercury intrusion and bubble point measurements of larger pore openings of woven geotextiles are questionable. However, it is important to note that modified bubble point equipment designed for highly permeable materials has accurately measured O_{95} values of woven polyester meshes in the range of 600 to 700 μm (Bhatia 1996).

3.2 Staple Fiber, Needle-Punched, Nonwoven Geotextile D1

The staple fiber, needle-punched, nonwoven geotextile, D1, also showed a wide range in O_{95} , O_{50} , and O_{15} values, as shown in Figure 2 and Table 4. However, the shapes of the pore-size distribution curves were much different from those for the slit-film, woven geotextile, A3. The mercury intrusion and image analysis methods gave the largest O_{95} values, while the bubble point method gave the smallest. The O_{95} results obtained using the sieving techniques fell between these two ranges. The shapes of the bubble point and mercury intrusion pore-size distribution curves were similar in that a fairly uniform pore-size distribution was obtained, whereas the image analysis resulted in a

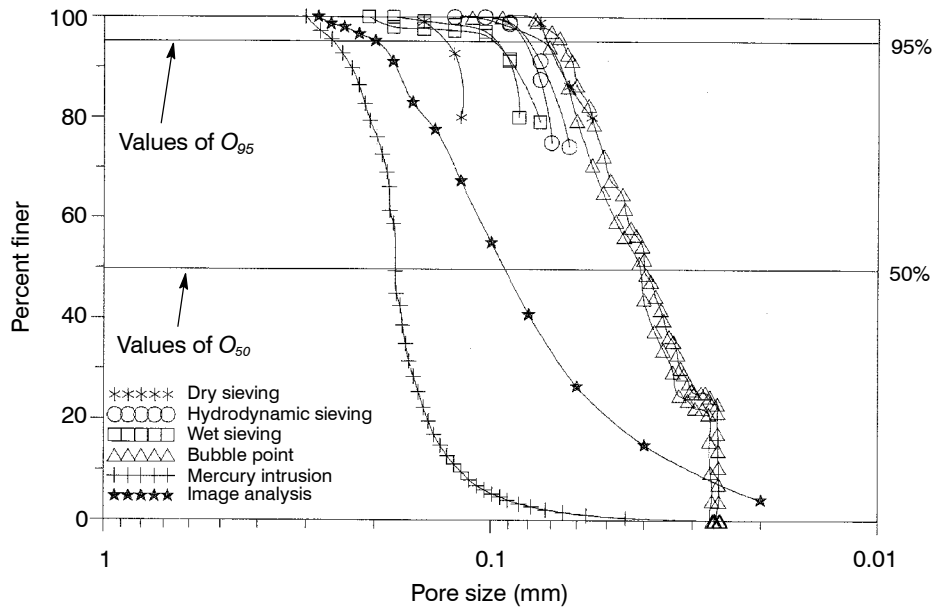


Figure 2. The complete pore-size distribution curves evaluated using each test method for staple fiber, needle-punched, nonwoven geotextile D1.

Table 4. Average pore opening results using different test methods for staple fiber, needle-punched, nonwoven geotextile D1.

Pore opening	Dry sieving (mm)	Wet sieving (mm)	Hydrodynamic sieving (mm)	Bubble point method (mm)	Mercury intrusion porosimetry (mm)	Image analysis (mm)
O_{95}	0.106	0.100	0.0850	0.0720	0.256	0.200
O_{50}	N/A	N/A	N/A	0.0406	0.177	0.0930
O_{15}	N/A	N/A	N/A	0.0260	0.140	0.0400

Note: N/A = not applicable.

well-graded distribution. Since the image analysis method is a technique for direct measurement of geotextile pore openings in two dimensions, the comparison is based on this method. Image analysis results also have some limitations (Bhatia et al. 1993) and are not necessarily a good indication of the filtration opening size, *FOS*, but this is the only technique which allows a somewhat direct measurement of the pores of a geotextile.

In comparison with image analysis results, mercury intrusion results were approximately 30% higher, whereas the sieving techniques and bubble point method were

approximately 55% lower than image analysis results. In terms of O_{50} values, mercury intrusion results were approximately 90% higher and bubble point results were approximately 55% lower than image analysis results. However, in the range of O_{15} values, mercury intrusion results were approximately 250% higher and bubble point results were approximately 35% lower.

3.3 Continuous Filament, Needle-Punched, Nonwoven Geotextile C3

The continuous filament, needle-punched nonwoven geotextile, C3, showed similar trends in O_{95} , O_{50} , and O_{15} values and shapes of pore-size distribution curves as the staple fiber geotextile, D1 (Figure 3 and Table 5). However, in this case the image analysis results gave the highest O_{95} values and the smallest O_{15} values. The mercury intrusion O_{15} results were approximately 15% lower and the dry sieving results were approximately 45% lower than the image analysis O_{95} values. Hydrodynamic sieving, wet sieving, and the bubble point method gave similar O_{95} results, being in the range of 65% to 70% lower than image analysis results. In terms of O_{50} values, mercury intrusion results were 105% higher and bubble point results were 50% lower than image analysis results. In terms of O_{15} values, mercury intrusion results were 350% higher than image analysis results.

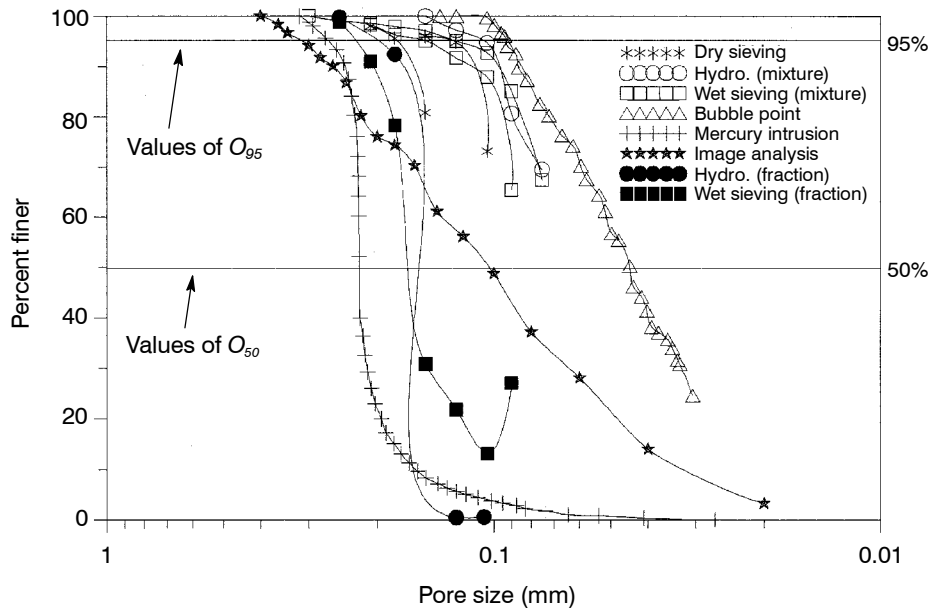


Figure 3. The complete pore-size distribution curves evaluated using each test method for continuous filament, needle-punched, nonwoven geotextile C3.

Note: Hydro. = hydrodynamic sieving.

Table 5. Average pore opening results using different test methods for continuous filament, needle-punched, nonwoven geotextile C3.

Pore opening	Dry sieving (mm)	Wet sieving (mm)		Hydrodynamic sieving (mm)		Bubble point method (mm)	Mercury intrusion porosimetry (mm)	Image analysis (mm)
		Mixture	Fraction	Mixture	Fraction			
O_{95}	0.170	0.114	0.230	0.112	0.230	0.103	0.257	0.312
O_{50}	N/A	N/A	0.180	N/A	0.180	0.0530	0.216	0.105
O_{15}	N/A	N/A	0.110	N/A	0.180	N/A	0.190	0.0414

Note: N/A = not applicable.

The hydrodynamic sieving method was conducted with glass bead mixtures, therefore, O_{50} and O_{15} results had no meaning, and because of this, a limited number of hydrodynamic sieving and wet sieving tests were also performed with glass bead fractions. These results are also given in Figure 3 and Table 5. It can be seen that the hydrodynamic and wet sieving tests using glass bead fractions are slightly larger than results given by the dry sieving method using fractions. The wet sieving results using glass bead fractions also indicate that agglomeration takes place during the test with fine glass bead particles. The effects of agglomeration with fine glass bead particles are similar to electrostatic effects observed in dry sieving tests, as shown in Part II (Bhatia and Smith 1996b).

3.4 Continuous Filament, Heat-Bonded, Nonwoven Geotextile E5

The continuous filament, heat-bonded geotextile results, E5, also showed a wide range in O_{95} values, however, the shapes of the pore-size distribution curves were different from any other type of geotextile, as shown in Figure 4 and Table 6. The most pronounced difference was the convergence of the mercury intrusion and bubble point results in the finer pore size range. Mercury intrusion O_{95} results were approximately 30% higher than image analysis results. Dry sieving results were approximately 30% lower, and wet sieving and hydrodynamic sieving results varied between 40 and 60% lower than image analysis results. Bubble point O_{95} results were approximately 50% less than image analysis results. In the range of O_{50} values, mercury intrusion results were approximately 100% higher, and bubble point results were approximately 40% lower. In the range of O_{15} values, mercury intrusion results were approximately 110% higher and bubble point results were comparable to the image analysis results.

Table 6. Average pore opening results using different test methods for continuous filament, heat-bonded, nonwoven geotextile E5.

Pore opening	Dry sieving (mm)	Wet sieving (mm)	Hydrodynamic sieving (mm)	Bubble point method (mm)	Mercury intrusion porosimetry (mm)	Image analysis (mm)
O_{95}	0.0970	0.0870	0.0550	0.0690	0.184	0.140
O_{50}	0.0620	N/A	N/A	0.0303	0.101	0.0500
O_{15}	N/A	N/A	N/A	0.0200	0.0460	0.0220

Note: N/A = not applicable.

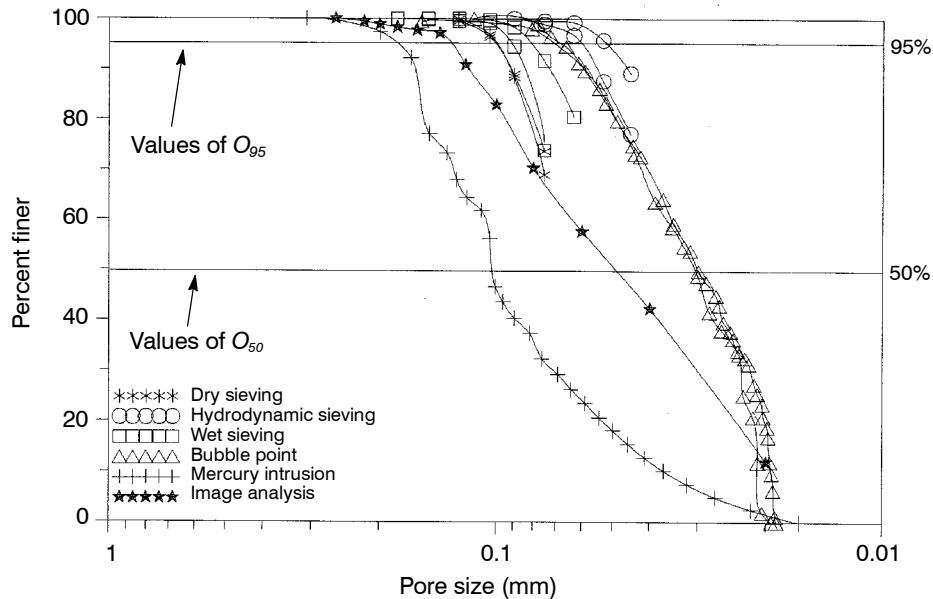


Figure 4. The complete pore-size distribution curves evaluated using each test method for continuous filament, heat-bonded, nonwoven geotextile E5.

4 DISCUSSION

The comparison of results clearly indicates that there are differences between pore-size distribution analysis methods. The differences in results arise due to complex geotextile pore structures and diverse test mechanisms.

4.1 Geotextile Pore Structure

4.1.1 Woven Geotextiles

Theoretically, a woven geotextile should have a uniform pore structure with little variability. This is not always the case due to the ability to alter the manufacturing process, such as the type of weave, and in some cases the non-uniformity of the weave, as shown in Part I (Bhatia and Smith 1996a). The dry sieving method gave predominantly one pore size in the woven geotextile, whereas the bubble point, mercury intrusion, and microscope methods resulted in a wide range of pore sizes in the geotextile. The bubble point and mercury intrusion methods also resulted in much smaller pore values in the geotextile, as opposed to the dry and hydrodynamic sieving methods.

There are several problems when using sieving techniques to evaluate the pore-size distribution of woven geotextiles. When glass beads (fractions or mixtures) are sieved through larger pore openings, most of the fine glass beads find the larger pore openings

and easily pass through the geotextile. This is why sieving techniques are generally only useful for evaluating the O_{95} pore openings of geotextiles. The larger pores can be measured, yet, the finer pores cannot, and therefore, a more uniform pore-size distribution is generally obtained even when it does not exist.

The bubble point and mercury intrusion porosimetry methods resulted in opposite trends than the sieving techniques. The bubble point method is ideally designed for fine pore materials and cannot effectively measure the large pores of woven geotextiles. Because the pore openings of the geotextiles are large in comparison with materials typically tested, the air flow required was at too high a volume and velocity for the instrument to accurately assess the sizes of the pores. However, it is important to note that new versions of such equipment may be better suited for materials with larger pore openings.

4.1.2 *Nonwoven Geotextiles*

Nonwoven geotextiles are made of randomly oriented fibers, thus there are no measurable pores within the structure. The nonwoven, staple fiber, needle-punched geotextile D1 (see Figure 2) and the nonwoven, continuous filament, needle-punched geotextile C3 (see Figure 3) of similar mass per unit area, showed similar pore-size distribution trends. The mercury intrusion and dry sieving methods resulted in predominantly one pore size for the nonwoven geotextiles. The image analysis method gave similar O_{95} results to the dry sieving and mercury intrusion methods; however, a larger range of pore sizes was obtained. The hydrodynamic sieving, wet sieving, and bubble point methods gave similar O_{95} trends for both nonwoven geotextiles.

4.2 Test Mechanisms

The pore-size distribution of a geotextile can be evaluated using one of several different methods. The meaning of the pore-size distribution results obtained is dependent on the method used. In this section, the methods are described in terms of physical meaning. With this comparison, the inherent differences between the methods and what they measure can be identified.

4.2.1 *Sieving Methods*

In dry sieving, glass bead fractions (from finer to coarser) are sieved through the geotextile. In theory, most of the glass beads from the first glass bead fraction should pass through the geotextile. As larger and larger glass bead fractions are sieved, more and more glass beads should become trapped within and on top of the geotextile. The number of pores of a certain size should be reflected by the percentage of glass beads passing through the geotextile during each glass bead fraction sieved; however, electrostatic effects between glass beads, and between glass beads and the geotextile can affect the results. Glass beads may stick to geotextile fibers making the pores effectively smaller and they may also agglomerate to form one large glass bead that is too large to pass through the geotextile. For example, 0.075 mm glass beads could effectively become one large particle equivalent to a diameter of 0.250 mm. Glass beads may also break

from hitting each other and the sides of the container, resulting in smaller particles that can pass through smaller openings.

In hydrodynamic sieving, a glass bead mixture is sieved through a geotextile under alternating water flow conditions. The use of glass bead mixtures leads to results that reflect the original glass bead mixture used. Therefore, this method is only useful for evaluating the larger pore openings of a geotextile, such as O_{95} (if the largest 5% of particles is larger than the largest pore openings in the geotextile). Another problem occurs when particles of many sizes interact, which likely results in particle blocking and bridge formation. This is especially a problem in hydrodynamic sieving because the larger glass bead particles will settle first when water is drained during the test. When this occurs, fine glass beads which are smaller than the pores of the geotextile are prevented from passing through the geotextile by the coarser particles.

In wet sieving, a glass bead mixture is sieved through a geotextile aided by a water spray. The same basic mechanisms that occur when using the hydrodynamic sieving method also occur when using the wet sieving method. Bridge formation is not as pronounced in the wet sieving method as in the hydrodynamic sieving method; however, particle blocking and glass bead agglomeration are more pronounced, as shown in Part II (Bhatia and Smith 1996b).

One of the major differences between dry sieving, and hydrodynamic and wet sieving methods is the use of fractions versus glass bead mixtures. A limited number of tests were performed on nonwoven geotextiles using both hydrodynamic and wet sieving methods with glass bead fractions (see Figure 3). Each point on the pore-size distribution curves shown in Figure 3 for glass bead fractions represents one test. The glass bead fraction results showed much larger pore openings as compared to results with glass bead mixtures for both wet and hydrodynamic sieving. However, the glass bead fraction results were similar to dry sieving test results, indicating that the difference between dry sieving, and wet and hydrodynamic sieving is due more to soil particle interaction than to static charge. This is true for the larger particle size range rather than the smaller.

The relationship between hydrodynamic and wet sieving results was linear. There was less scatter in O_{95} values smaller than 0.25 mm, and more for O_{95} values larger than 0.25 mm. The O_{95} results for dry sieving are systematically higher than those for hydrodynamic and wet sieving. For design purposes, dry sieving results can be related to hydrodynamic and wet sieving results for the types of geotextiles tested, in the range of 0.25 mm and lower (Bhatia and Smith 1996b).

4.2.2 *Bubble Point Method*

The bubble point method is a dynamic test where continuous air flow is used to remove liquid from the pores of a geotextile. Since air flow is only applied to one side of the geotextile, liquid is removed from those pores which form a continuous path through the geotextile. These pores are emptied of liquid in order from largest to smallest. Since it is a flow through technique, the bubble point method measures the narrowest diameter of each pore channel present in the geotextile (see Bhatia and Smith 1995). This method provides information on the number and sizes of the smallest effective flow through pore channels in a geotextile.

4.2.3 *Mercury Intrusion Porosimetry*

The mercury intrusion porosimetry test, as opposed to the bubble point method, is a static test. The pores of the geotextile are not measured as continuous pore channels through the geotextile, but as singular pores within the geotextile (e.g. Bhatia and Smith 1994). These pores are measured from largest to smallest in terms of total pore volume. Mercury will intrude the pores of a geotextile from all directions as the pressure is increased. Once mercury fills a pore, the test in that section of the pore channel stops. Any dead-end pores or crevices between fibers which are not part of the continuous path through the geotextile, in addition to those which extend through the geotextile, are measured. The mercury intrusion method thus gives a pore-size distribution based on total pore volume and gives no information regarding the number of pores or pore constrictions of a geotextile.

4.2.4 *Image Analysis and Microscopic Methods*

Image analysis and microscopic methods can both be used to directly measure the pore openings in a geotextile. Image analysis is based on direct measurements made in the cross-section of the geotextile. Many investigators (e.g. Lombard and Rollin 1987; Bhatia et al. 1990; Bhatia et al. 1991) have used this technique to characterize pore-size distribution. The measurements are then projected in the third dimension to evaluate pore-size distribution.

The pore openings of slit-film woven geotextiles can be directly measured with a microscope in plan view. By measuring the length and width of pore openings, the effective circular diameters can be calculated. The effective diameter was based on the smaller of the two measurements taken for each pore opening. Fifty pore openings were measured for each geotextile specimen. The frequency of occurrence of each size pore was used to evaluate the pore-size distribution.

4.3 **Comparison of Characteristic Pore Sizes**

Since several geotextiles manufactured by the same manufacturer varied in thickness or mass per unit area, the O_{95} and O_{50} results obtained were compared as a function of thickness for the nonwoven geotextiles only. The woven geotextiles showed no significant trends in opening sizes and a large scatter in results, and are therefore not included. Since mercury intrusion porosimetry only gives results in terms of pore volume, mercury intrusion results are also not included in these comparisons.

4.3.1 *Comparison of O_{95} and Its Relationship with Thickness*

The nonwoven, needle-punched, staple fiber geotextile O_{95} results versus thickness are given in Figure 5a. The largest scatter of data between the different methods occurred for the thinner geotextiles. The thinner nonwoven geotextiles displayed a higher degree of variability, as opposed to thicker, denser geotextiles due to the fewer number of fibers. The dry sieving method resulted in a good trend of decreasing opening size with increasing thickness. The bubble point results were repeatable, however, there was little effect of thickness on opening size. The hydrodynamic and wet sieving technique

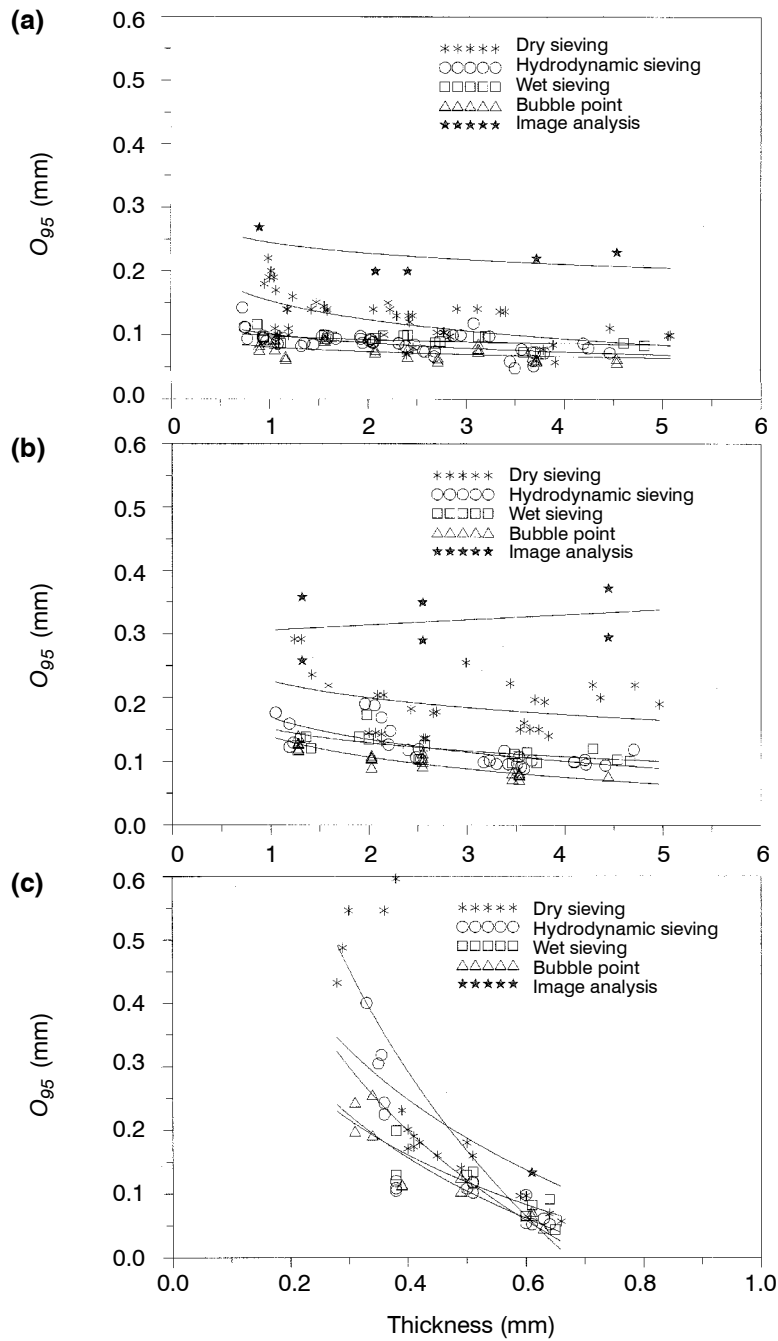


Figure 5. O_{95} test results versus thickness: (a) staple fiber, needle-punched geotextiles; (b) continuous filament, needle-punched geotextiles; (c) continuous filament, heat-bonded geotextiles.

results for O_{95} values were very similar in all cases, with little variation in values due to geotextile thickness.

The nonwoven, needle-punched, continuous filament geotextile O_{95} results versus thickness are given in Figure 5b. The most noticeable feature from this comparison is the large difference in results between different methods. The hydrodynamic and wet sieving methods again gave similar results. The dry sieving method also gave very large O_{95} results as compared to the results obtained using the other methods.

The nonwoven, heat-bonded, continuous filament geotextile O_{95} results versus thickness are given in Figure 5c. The thinner heat-bonded geotextiles showed the largest scatter in O_{95} results, when compared to the thicker heat-bonded geotextiles shown in Figure 5c. The hydrodynamic sieving, wet sieving, and bubble point methods showed similar trends in opening size with increasing thickness for the heat-bonded geotextiles. The woven geotextiles showed no significant trends and a large scatter in O_{95} results.

Giroud (1996) gives a relationship that presents the FOS of a nonwoven geotextile as a function of porosity, fiber diameter and thickness. Using average properties given in Table 1, opening sizes were calculated for the nonwoven, needle-punched geotextiles (B1-B5, C1-C6, D1-D5) based on the relationship given by Giroud (1996). These results are plotted as a function of thickness in Figure 6. As shown in Figure 6, the calculated FOS values decrease as a function of increasing geotextile thickness. This relationship is similar to results shown in Figure 5a for staple fiber geotextiles and Figure 5b for continuous filament geotextiles; however, for thinner geotextiles (less than 3 mm) the calculated opening sizes are larger than O_{95} values obtained by hydrodynamic sieving and smaller than those values obtained by dry sieving.

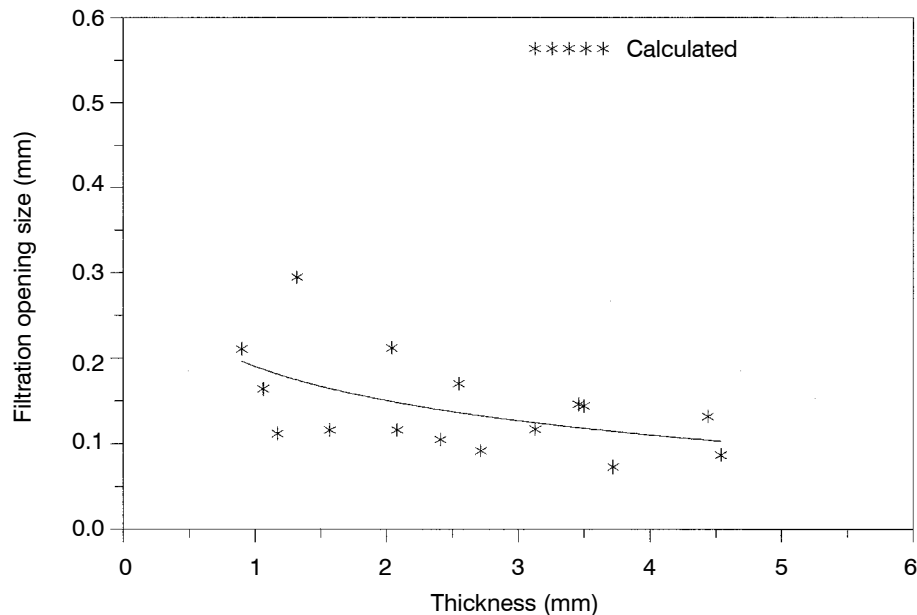


Figure 6. Calculated filtration opening size, FOS , test results versus thickness for geotextiles B1-B5, C1-C6, and D1-D5 based on the relationship given by Giroud (1996).

4.3.2 Comparison of O_{50} and Its Relationship with Thickness

The nonwoven, needle-punched, staple fiber geotextile O_{50} results versus thickness are given in Figure 7a. O_{50} results were fairly repeatable for the methods used. The image analysis and bubble point method results showed similar decreasing O_{50} value trends with increasing thickness. The image analysis O_{50} results were, however, much higher than the bubble point results.

The nonwoven, needle-punched, continuous filament geotextile O_{50} results versus thickness are given in Figure 7b. In general, similar trends were found with these geotextiles as with the staple fiber geotextiles. The scatter in O_{50} results is slightly greater, yet, the results are similar.

The nonwoven, heat-bonded, continuous filament geotextiles O_{50} results versus thickness are given in Figure 7c. The bubble point method showed decreasing O_{50} values with increasing geotextile thickness.

5 FILTER DESIGN EXAMPLE

5.1 Introduction

Although there are established retention, permeability, and clogging criteria available for the designer, the criteria in general are not straightforward and are misleading. Assuming that the criteria are fairly good indicators of the retention ability of a geotextile with a particular soil, there are two general fundamental problems with the criteria. First, some criteria require pore sizes of the geotextile that are not generally evaluated such as O_{50} and O_{15} values. As discussed in Part II (Bhatia and Smith 1996b), there are no ideally suited methods for evaluating these pore sizes of a geotextile. Second, the opening sizes (O_{95} and O_{90}) can be evaluated using many different methods that yield differing results for a particular geotextile. Most of the design methods have been empirically verified based on the results of a single method (dry sieving or hydrodynamic sieving). If a designer uses pore opening results from another method, results may be incorrect. A comparison of the results from dry sieving, wet sieving, hydrodynamic sieving, mercury intrusion porosimetry, bubble point method, and image analysis tests presented in this paper shows the wide range of O_{95} or O_{90} values that can be obtained for a given geotextile. The following design example illustrates the differences in pore opening values obtained by the six methods.

5.2 Example

The ABC Construction Company was contracted to build a temporary tunnel, approximately 3.1 m in diameter, for a sewer line system. During the initial construction stage, the contractor installed a thin nonwoven geotextile with an AOS value of 0.21 mm as a tunnel liner. A substantial amount of soil washed through the geotextile, and the company stopped the project, fearing a collapse of the tunnel.

The ABC Construction Company wanted to select a suitable nonwoven geotextile as a temporary liner material for the tunnel. The construction company suggested three possible nonwoven geotextiles as candidates (C4, D4 and E5) (see Table 1).

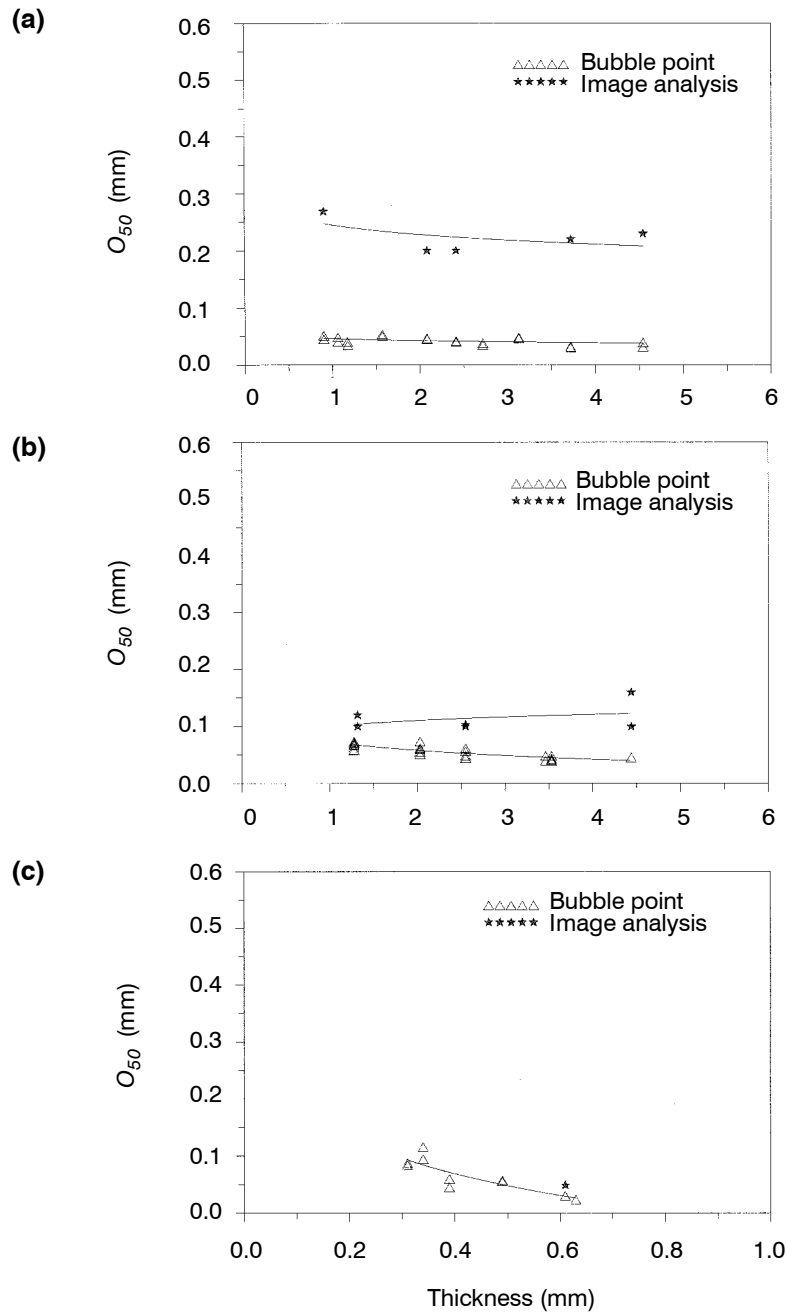


Figure 7. O_{50} test results versus thickness: (a) staple fiber, needle-punched geotextiles; (b) continuous filament, needle-punched geotextiles; (c) continuous filament, heat-bonded geotextiles.

Limited information about the site was available (see Figure 8). The particle-size distribution of the silt surrounding the geotextile is shown in Figure 9. The soil parameters that were obtained from the particle-size distribution curve are given in Table 7.

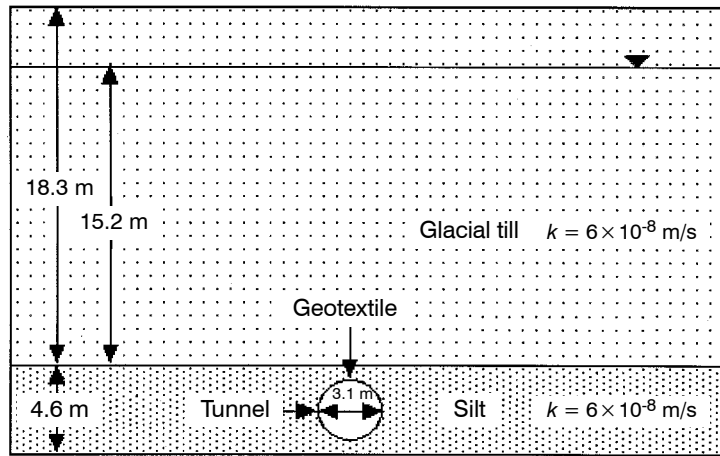


Figure 8. Schematic of the tunnel.

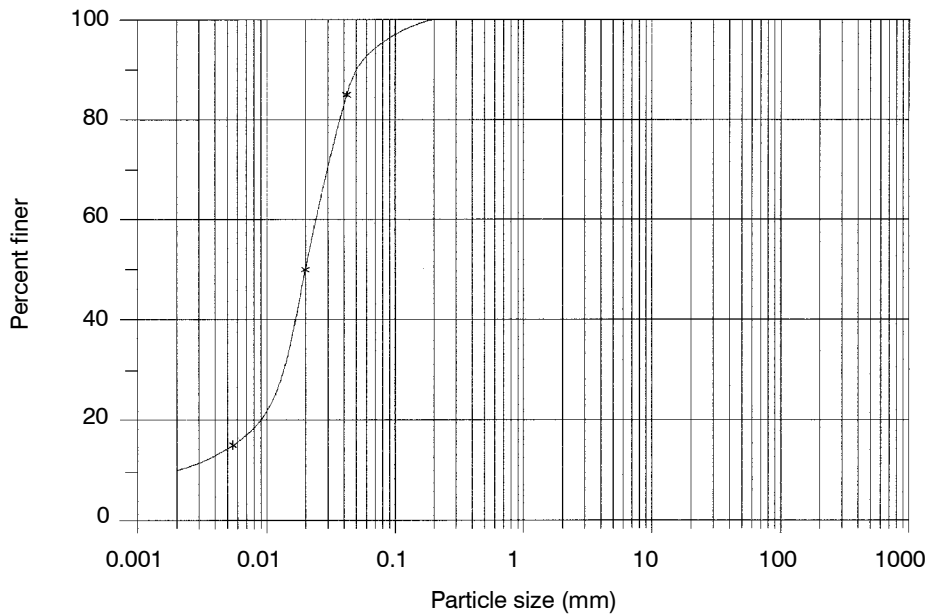


Figure 9. Particle-size distribution of the silt surrounding the tunnel.

Table 7. The soil parameters of the silt obtained from the particle-size distribution curve shown in Figure 8.

Soil parameter	Value
d_{85}	0.042 mm
d_{50}	0.02 mm
d_{15}	0.0055 mm
C_u	12.5
C_c	4.5
C'_u	2.93

Notes: d_x = soil particle size for which x percent is smaller; C_u = soil coefficient of uniformity = d_{60}/d_{10} ; C_c = soil coefficient of curvature = $(d_{30})^2/(d_{10} \times d_{60})$; C'_u = soil linear coefficient of uniformity = $(d'_{100}/d'_0)^{0.5}$.

5.3 Solution

The geotextile in this example must work as a filter; therefore, it must satisfy retention, permeability and clogging criteria. To design a geotextile as a filter, information regarding the largest effective pore opening (O_{95}) and permeability of the geotextile must be known. Therefore, the first step of the design is to determine these properties.

Step 1 - Property Determination

For the geotextiles selected (C4, D4, and E5), dry sieving, hydrodynamic sieving, wet sieving, bubble point, mercury intrusion, and image analysis tests were performed to determine the pore-size distribution of the geotextiles. In addition, permeability tests were conducted following ASTM D 4491. The permeability of geotextiles C4, D4, and E5 is 0.0035, 0.0013 and 0.00037 m/s, respectively, as shown in Table 8.

Step 2 - Retention Criteria

The flow conditions in this case are unidirectional, therefore, only retention criteria based on unidirectional flow conditions are considered. For this design, four filter criteria based on the O_{95} value will be applied (Giroud 1982; Carroll 1983; Christopher and Holtz 1985; Bhatia et al. 1990). Criteria based on geotextile pore openings other than the O_{95} value were not considered due to the difficulties in measuring the smaller pore openings, as discussed in Part II (Bhatia and Smith 1996b). Even so, in evaluating the requirements with respect to pore size, it should be noted that all of the criteria, with the exception of Bhatia et. al (1990), do not specify the use of the O_{95} value by dry or hydrodynamic sieving procedures. However, it is general practice, if not specified, to use the O_{95} value taken from the dry sieving method.

Table 8. The opening size and permeability properties of the candidate geotextiles.

Method	Geotextile C4	Geotextile D4	Geotextile E5
Dry sieving O_{95} (mm)	0.150	0.143	0.0970
Hydrodynamic sieving O_{95} (mm)	0.0960	0.0960	0.0550
Wet sieving O_{95} (mm)	0.0980	0.0990	0.0870
Bubble point method O_{95} (mm)	0.0780	0.0920	0.0690
Mercury intrusion porosimetry O_{95} (mm)	0.244	0.245	0.184
Image analysis O_{95} (mm)	0.390	0.240	0.140
Permeability (m/s)	3.5×10^{-3}	1.3×10^{-3}	3.7×10^{-4}

Table 9. Geotextile retention criteria test results.

Retention criteria	Required geotextile O_{95} (mm)
Giroud (1982) $O_{95}/d_{50} < 9/C'_u$ to $18/C'_u$	< 0.0614 - 0.123
Carroll (1983) $O_{95}/d_{85} < 2$ to 3	< 0.0840 - 0.126
Christopher and Holtz (1985) $O_{95}/d_{85} < 1.8$ for nonwovens > 50% fines	< 0.0756
Bhatia et al. (1990) $FOS/d_{85} < 3$	< 0.126

The critical O_{95} pore size was calculated for each of the criteria. These values are given in Table 9. For the following discussion only dry and hydrodynamic sieving results were used since these values are most often used by designers today. As shown in Table 9, the retention criteria requires that the geotextile O_{95} value be less than the range of 0.0614 mm (Giroud 1982) to 0.126 mm (Bhatia et al. 1990; Carroll 1983) to prevent the silt from washing into the tunnel at the site.

Based on dry sieving results, none of the geotextiles passed the Christopher and Holtz (1985) criteria. However, for medium dense to dense silts, geotextile E5 passed the Giroud and Carroll criteria. When hydrodynamic sieving O_{95} results were used, all three geotextiles passed the Giroud, Carroll, and the Bhatia et al. criteria. Only geotextile E5 passed the Christopher and Holtz criteria when hydrodynamic sieving O_{95} results were used.

Therefore, the same geotextiles can pass or fail a design criteria by merely using dry or hydrodynamic sieving test results and some geotextiles can be acceptable or unacceptable based on the design criteria.

Step 3 - Permeability Criteria

The permeability of the silt surrounding the tunnel was estimated to be 10^{-8} m/s using Figure 10 under moderate confining stress conditions. The existing permeability criteria require the permeability of the geotextile to be at least ten times greater than the permeability of the soil. As indicated in Table 8, the geotextiles have a permeability in

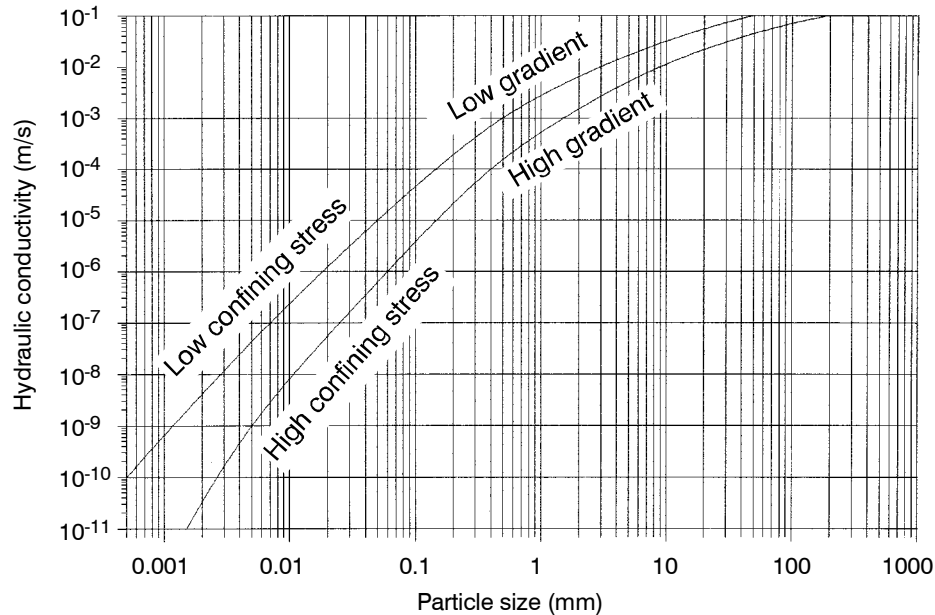


Figure 10. Typical hydraulic conductivity values (after Luettich 1992).

the range of 3.7×10^{-4} to 3.5×10^{-3} m/s, which is several orders of magnitude higher than the permeability of the soil; therefore, the geotextiles satisfy the permeability criteria.

Step 4 - Clogging Criteria

It was suggested that, for critical applications, performance tests should be conducted; therefore, long-term filtration (LTF) tests were performed using the silt from the site and the candidate geotextiles. The purpose of the LTF tests was to evaluate the compatibility of the three nonwoven geotextiles with the silt provided from the site.

The site soil was classified under the Unified Soil Classification System (USCS) as a silt with low liquid limit (ML) and a uniformity coefficient (C_u) of 12.5. Ninety-six percent of the particles of this soil were finer than 0.075 mm (U.S. Standard Sieve Number 200). The 3.1 m tunnel opening, which was 21.3 m below the ground surface, was to be lined with a nonwoven geotextile. Since the opening was surrounded by a 0.9 to 1.5 m thick layer of silt, there was some concern that under high hydraulic gradient conditions, an excessive amount of silt may wash through the geotextile, thus creating unfavorable conditions for the proposed construction. For this reason, the anticipated high hydraulic gradients were calculated prior to conducting the LTF tests.

Calculation of Hydraulic Gradient In order to determine an upper bound value of the maximum possible hydraulic gradient, i , for the proposed construction site, the following assumptions about the site conditions were made:

- The tunnel has a 1.5 m radius, r .
- The permeability, k , of the surrounding glacial till and the silt layer is similar, 10^{-7} to 10^{-8} m/s.
- The ground water table is 19.8 m above the center of the tunnel (see Figure 11; assume the head at radius r to be h).

For a tunnel length, l , the maximum hydraulic gradient was calculated as follows:

$$v = k i = k (dh/dr) \quad (1)$$

$$q = 2 \pi r l k (dh/dr) \quad (2)$$

$$(dr/r) = (2 \pi l k) dh/q \quad (3)$$

Integrating the above equation over the region:

$$\ln(R/r_i) = 2 \pi l k (h_o - h_i)/q \quad (4)$$

$$q = 2 \pi l k (h_o - h_i)/\ln(R/r_i) \quad (5)$$

By comparing Equations 2 and 5:

$$i = (dh/dr) = [(h_o - h_i)/\ln(R/r_i)]/r \quad (6)$$

If $h_i = 0$, $h_o = 18.3$ m, $r_i = 1.5$ m, $R = 19.8$ m, the maximum hydraulic gradient will be:

$$i_{max} = [(18.3 - 0)/\ln(19.8/1.5)]/1.5 = 4.7 \quad (7)$$

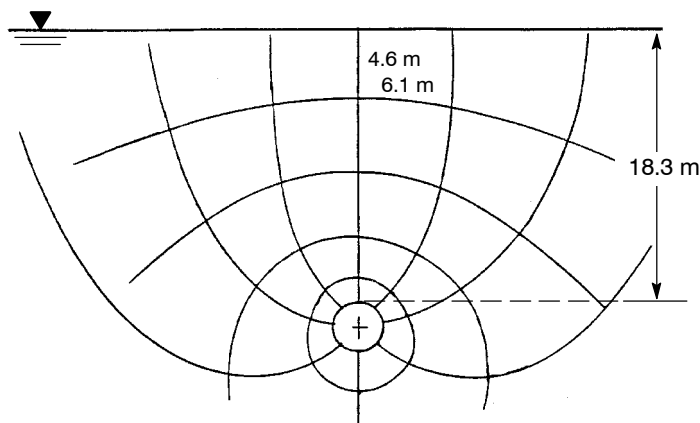


Figure 11. Flownet for the design tunnel.

The maximum hydraulic gradient was also calculated by constructing a flownet. For calculating the flownet, it was assumed that the permeabilities of the till and silt layers were the same. For trench excavations in nonhomogeneous soils with unconfined flow:

$$dh = h_o / (4 + \cot\beta) \quad (8)$$

If, $h_o = 18.3$ m and $\cot\beta = 4.6/6.1$ (from Figure 11), then:

$$dh = 18.3 / (4 + 4.6/6.1) = 3.9 \text{ m} \quad (9)$$

If the radius of the tunnel is 1.5 m, the maximum hydraulic gradient is as follows:

$$i_{max} = (dh/dr)_{max} = 3.9/1.5 = 2.6 \quad (10)$$

The first technique resulted in higher hydraulic gradient values (4.7) than the flownet method (2.6). By using a factor of safety of 2, the proposed hydraulic gradient set for this project was 9.4. It was therefore decided to perform the LTF tests using a hydraulic gradient of 10.

Long-Term Filtration Tests in the Laboratory Several LTF tests were performed. The geotextiles were saturated in the permeameter and a silt soil (slurry with a moisture content of 45%) was placed on top of the specimens. A hydraulic gradient of 10 was applied. Initially, some fines piped through the geotextiles, but the systems typically stabilized within one day. The flow rate was monitored every 15 minutes for 300 hours. The test results for the three geotextiles with the silt soil are shown in Figure 12. Piping was not observed through any of the geotextiles tested. The small amount of fines that did pass was far below the threshold value of 2500 g/m² proposed by Lafleur et al. (1989).

Long-Term Filtration Performance of Geotextile as a Filter in the Field There are numerous other factors such as compressibility of the geotextile, hydraulic characteristics of the water flow, and clogging of the geotextile due to chemicals which could affect the performance of the geotextile as a filter. This design illustrates only one aspect, that is, pore-size characterization of geotextiles in isolation. Designers should consider all other factors in the design of geotextiles as filters.

Step 5 - Conclusions

Based on the LTF tests, all three geotextiles would perform satisfactorily as the filter for the temporary tunnel. Although the geotextiles had varying pore-size distributions as evaluated using the six different methods, they exhibited similar flow behavior and filtration performance during the LTF tests. Piping was not apparent through any of the geotextiles during the tests.

Despite the satisfactory performance of the geotextiles in the laboratory LTF tests, the geotextiles were seen to pass or fail a design criteria by merely using dry or hydrodynamic sieving results. This observation indicates that existing retention criteria are conservative, some more so than others. It must also be considered that there are numerous

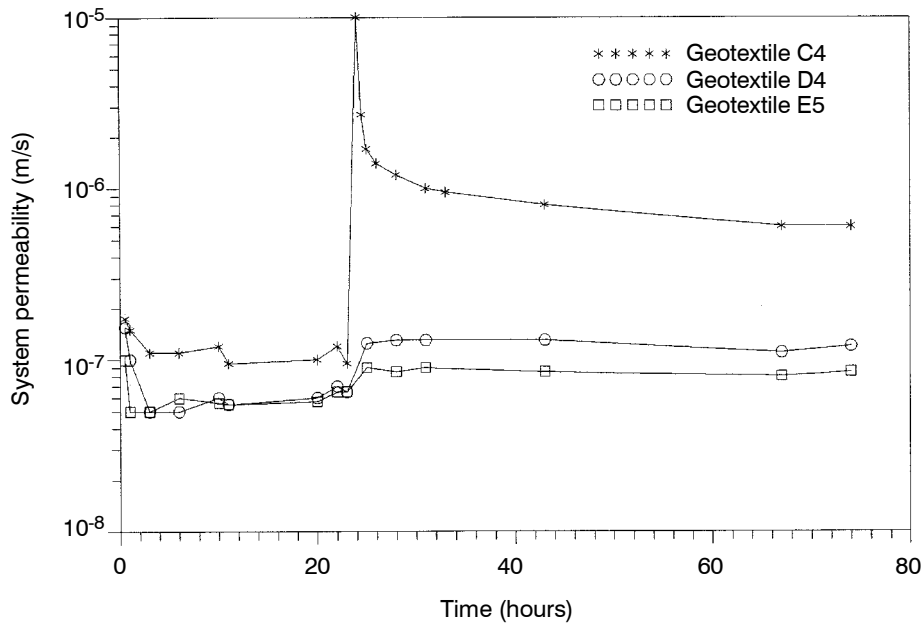


Figure 12. Results of geotextile system permeability tests versus time during an increase in hydraulic gradient from 4.2 to 10.

other factors such as compressibility, hydraulic characteristics of the water flow, and clogging that can affect the performance of a geotextile as a filter.

6 CONCLUSIONS

For all geotextiles, the pore sizes evaluated using the different methods were quite different. The pore-size distribution measured by these techniques for a particular geotextile is dependent on the test used for the evaluation as opposed to being a unique property of the geotextile.

The pore-size distribution test methods may give very similar or very different results. It is critical that the actual mechanism of a test and the geotextile structure being tested are known before the results of a test can be correctly used for a filter criteria.

In general, the dry sieving method shows a larger pore structure than the hydrodynamic and wet sieving methods, whose results are similar. An important difference between these tests is that the dry sieving technique is performed with glass bead fractions and the hydrodynamic and wet sieving tests are performed with glass bead mixtures. The bubble point and mercury intrusion porosimetry methods give very different results. The bubble point method gives information on the number and sizes of the smallest effective pore channels in a geotextile. The mercury intrusion porosimetry method only gives results in terms of pore volume and cannot be compared to the results obtained using the other methods.

The dry sieving method gives a reasonably good estimation of the largest effective opening in a geotextile (AOS), when the pore size is in a range larger than approximately 0.125 mm. In general, the O_{95} dry sieving results are much larger than the results obtained using the other methods.

The hydrodynamic sieving method gives a fairly good estimation of the largest effective FOS of a geotextile. The results are affected by the interaction of particles within the gradation. When glass bead mixtures are sieved, results beyond O_{95} are meaningless. O_{50} and O_{15} results can be obtained when fractions are used as the testing particles. In the range of O_{50} and O_{15} values, hydrodynamic sieving results are similar to dry sieving results obtained by sieving fractions.

The wet sieving method also uses a glass bead mixture. The pore-size distribution results were fairly repeatable, however, glass bead agglomeration was prominent. Since a glass bead mixture is also used in this test, results are meaningless beyond O_{95} . O_{50} and O_{15} results can also be obtained by sieving fractions. In the range of 0.125 mm, glass bead agglomeration effects were similar to electrostatic effects in the dry sieving test.

The bubble point method gives repeatable pore-size distribution results, however, there is little difference in results for geotextiles of various thicknesses. This especially holds true for needle-punched geotextiles, where air flow will find the largest pore channels of the geotextile, which should be very similar for a particular manufacturing process. This method does, however, show differences in pore-size distribution between heat-bonded geotextiles of various thicknesses. This is due to melding of fibers in the heat-bonding process. The bubble point method is also based on the assumption that the pores of the geotextile are cylindrical.

When the mass per unit area and thickness of the geotextiles were related to O_{95} values, the dry sieving, hydrodynamic sieving, wet sieving and bubble point method gave similar decreasing O_{95} value relationships with increasing mass per unit area and thickness for nonwoven geotextiles. However, these trends did not appear for woven geotextiles.

The design example further illustrates the differences between design criteria. Designers must be aware that there are numerous other factors that can affect the performance of a geotextile as a filter.

7 RECOMMENDATIONS

A standard test method for evaluating the pore-size distribution of a geotextile must be accepted world-wide. The test method selected must be carefully standardized to achieve the highest degree of reproducibility and must be appropriate for all types of geotextiles. Until this point is reached, knowledge of the test method used for pore-size determination and all of its variables is essential. In addition, it is critical that the results of this test method are only applied to filter criteria which are based on the test method.

Based upon results from this study, for the retention criteria, where the larger pores of the geotextile are critical, the microscope or dry sieving methods may be appropriate for woven geotextiles but are inadequate for nonwoven geotextiles. Hydrodynamic sieving or wet sieving would appear to be more appropriate for evaluating nonwoven geotextiles. The bubble point method may also be suitable but additional research is

required. The bubble point method appears to be promising for developing clogging criteria, where fine pores are more critical.

Once a world-wide pore-size distribution method is selected, pore-size distribution data for the different types of geotextiles must be related to the performance of a geotextile, with different types of soils under various conditions, in filtration performance tests.

ACKNOWLEDGMENTS

Research support from the National Science Foundation and the federally sponsored Patricia Harris Fellowship program is gratefully acknowledged. We would also like to thank Mr. B. Hawkins and Dr. J. Mlynarek for their support and assistance. The authors are most grateful for Dr. J.P. Giroud's constructive comments on this paper.

REFERENCES

- ASTM D 1777, "*Standard Test Method for Measuring Thickness of Textile Materials*", American Society for Testing and Materials, West Conshohocken, Pennsylvania, USA.
- ASTM D 3776, "*Standard Test Methods for Mass Per Unit Area (Weight) of Woven Fabric*", American Society for Testing and Materials, West Conshohocken, Pennsylvania, USA.
- ASTM D 4491, "*Standard Test Methods for Water Permeability of Geotextiles by Permittivity*", American Society for Testing and Materials, West Conshohocken, Pennsylvania, USA.
- ASTM D 4751, "*Standard Test Method for Determining Apparent Opening Size of a Geotextile*", American Society for Testing and Materials, West Conshohocken, Pennsylvania, USA.
- Bhatia, S.K., 1996, "*Bubble Point Test Results for Woven Polyester Mesh*", Syracuse University Report (complete report not available).
- Bhatia, S.K., Huang, Q. and Smith, J., 1993, "Application of Digital Image Processing in Morphological Analysis of Geotextiles", *Proceedings of Conference on Digital Image Processing: Techniques and Applications in Civil Engineering*, ASCE, proceedings of a symposium held in Kona, Hawaii, USA, February-March 1993, pp. 95-108.
- Bhatia, S.K., Mlynarek, J., Lafleur, J. and Rollin, A., 1991, "Influence of Microstructure on the Performance of Geotextiles", *Proceedings of Geosynthetics '91*, IFAI, Vol. 2, Atlanta, Georgia, USA, March 1991, pp. 629-642.
- Bhatia, S.K., Qureshi, S. and Kogler, R.M., 1990, "Long-Term Clogging Behavior of Nonwoven Geotextiles with Silty and Gap-Graded Sands", *Geosynthetic Testing for Waste Containment Applications*, Koerner, R.M., Editor, ASTM Special Technical Publication 1081, proceedings of a symposium held in Las Vegas, Nevada, USA, January 1990, pp. 285-298.

- Bhatia, S.K. and Smith, J.L., 1995, "Application of the Bubble Point Method to the Characterization of the Pore-Size Distribution of Geotextiles", *ASTM Geotechnical Testing Journal*, Vol. 18, No. 1, pp. 94-105.
- Bhatia, S.K. and Smith, J.L., 1994, "Comparative Study of Bubble Point Method and Mercury Intrusion Porosimetry Techniques for Characterizing the Pore-Size Distribution of Geotextiles", *Geotextiles and Geomembranes*, Vol. 13, No. 10, pp. 679-702.
- Bhatia, S.K. and Smith, J.L., 1996a, "Geotextile Characterization and Pore-Size Distribution: Part I. A Review of Manufacturing Processes", *Geosynthetics International*, Vol. 3, No. 1, pp. 85-105.
- Bhatia, S.K. and Smith, J.L., 1996b, "Geotextile Characterization and Pore-Size Distribution: Part II. A Review of Test Methods and Results", *Geosynthetics International*, Vol. 3, No. 2, pp. 155-180.
- Bhatia, S.K. Smith, J.L. and Christopher, B., 1994, "Interrelationship Between Pore Openings of Geotextiles and Methods of Evaluation", *Proceedings of the Fifth International Conference on Geotextiles, Geomembranes and Related Products*, Vol. 2, Singapore, September 1994, pp. 705-710.
- Carroll, R.G., Jr., 1983, "Geotextile Filter Criteria", *Transportation Research Record* 916, Washington, DC, USA, pp. 46-53.
- Christopher, B.R. and Holtz, R.D., 1985, "*Geotextile Engineering Manual*", U.S. Department of Transportation, Federal Highway Administration, Washington, DC, USA, Report No. FHWA-TS-86/203, March 1985, 1044 p.
- Fischer, G.R., Holtz, R.D. and Christopher, B.R., 1996, "Characteristics of Geotextile Pore Structure", *Recent Developments in Geotextile Filters and Prefabricated Drainage Geocomposites*, Bhatia, S.K. and Suits, L.D., Editors, ASTM Special Technical Publication 1281, proceedings of a symposium held in Denver, Colorado, USA, June 1995, pp. 3-18.
- Giroud, J.P., 1982, "Filter Criteria for Geotextiles", *Proceedings of the Second International Conference on Geotextiles*, IFAI, Vol. 1, Las Vegas, Nevada, USA, August 1982, pp. 103-108.
- Giroud, J.P., 1996, "Granular Filters and Geotextile Filters", *Proceedings of Geofilters '96*, Montreal, Quebec, Canada, May 1996, pp. 565-680.
- Lafleur, J., Mlynarek, J. and Rollin, A.L., 1989, "Filtration of Broadly Graded Cohesionless Soils", *Journal of Geotechnical Engineering*, Vol. 115, No. 12, pp. 1747-1748.
- Lombard, G. and Rollin, A., 1987, "Filtration Behavior Analysis of Thin Heat Bonded Geotextiles", *Proceedings of Geosynthetics '87*, IFAI, Vol. 2, New Orleans, Louisiana, USA, February 1987, pp. 482-492.
- Luetlich, S.M., Giroud, J.P. and Bachus, R.C., 1992, "Geotextile Filter Design Guide", *Geotextiles and Geomembranes*, Vol. 11, Nos. 4 - 6, pp. 355-370.

NOTATIONS

Basic SI units are given in parentheses.

AOS	=	apparent opening size (m)
C_c	=	coefficient of curvature, $(d_{30})^2/(d_{10} \times d_{60})$ (dimensionless)
C_u	=	coefficient of uniformity, d_{60}/d_{10} (dimensionless)
C'_u	=	linear coefficient of uniformity $(d'_{100}/d'_0)^{0.5}$ (dimensionless)
d_x	=	soil particle size for which $x\%$ of the sample is smaller (m)
d'_{100}, d'_0	=	equivalent d_{100} and d_0 obtained from the straight line approximation of the particle-size distribution curve (m)
FOS	=	filtration opening size (m)
h	=	hydraulic head at radius, r (m)
h_l	=	hydraulic head at the ground water table (m)
h_o	=	hydraulic head at the center of the tunnel opening, $r = 0$ (m)
i	=	hydraulic gradient (dimensionless)
i_{max}	=	maximum hydraulic gradient (dimensionless)
k	=	permeability of soil (m/s)
l	=	length of tunnel (m)
O_{15}	=	geotextile opening size such that 15% of pores are smaller than that size (m)
O_{50}	=	geotextile opening size such that 50% of pores are smaller than that size (m)
O_{90}	=	geotextile opening size such that 90% of pores are smaller than that size (m)
O_{95}	=	geotextile opening size such that 95% of pores are smaller than that size (m)
q	=	flow rate (m^3/s)
R	=	distance from the ground water table to the center of the tunnel (m)
r, r_l	=	radius of tunnel opening (m)
v	=	velocity of flow (m/s)
β	=	slope angle ($^\circ$)

ABBREVIATIONS

PP:	polypropylene
PET:	polyester
LTF:	long term filtration
USCS:	Unified Soil Classification System